



**HAL**  
open science

## **Megafloods in Europe can be anticipated from observations in hydrologically similar catchments**

Miriam Bertola, Günter Blöschl, Milon Bohac, Marco Borga, Attilio Castellarin, Giovanni B Chirico, Pierluigi Claps, Eleonora Dallan, Irina Danilovich, Daniele Ganora, et al.

### ► To cite this version:

Miriam Bertola, Günter Blöschl, Milon Bohac, Marco Borga, Attilio Castellarin, et al.. Megafloods in Europe can be anticipated from observations in hydrologically similar catchments. *Nature Geoscience*, 2023, 16, pp.982-988. 10.1038/s41561-023-01300-5 . hal-04344730

**HAL Id: hal-04344730**

**<https://hal.inrae.fr/hal-04344730>**

Submitted on 14 Dec 2023

**HAL** is a multi-disciplinary open access archive for the deposit and dissemination of scientific research documents, whether they are published or not. The documents may come from teaching and research institutions in France or abroad, or from public or private research centers.

L'archive ouverte pluridisciplinaire **HAL**, est destinée au dépôt et à la diffusion de documents scientifiques de niveau recherche, publiés ou non, émanant des établissements d'enseignement et de recherche français ou étrangers, des laboratoires publics ou privés.

# Megafloods in Europe can be anticipated from observations in hydrologically similar catchments

## Author list

Miriam Bertola<sup>1\*</sup>, Günter Blöschl<sup>1</sup>, Milon Bohac<sup>2</sup>, Marco Borga<sup>3</sup>, Attilio Castellarin<sup>4</sup>, Giovanni B. Chirico<sup>5</sup>, Pierluigi Claps<sup>6</sup>, Eleonora Dallan<sup>3</sup>, Irina Danilovich<sup>7</sup>, Daniele Ganora<sup>6</sup>, Liudmyla Gorbachova<sup>8</sup>, Ondrej Ledvinka<sup>2,9</sup>, Maria Mavrova-Guirguinova<sup>10</sup>, Alberto Montanari<sup>4</sup>, Valeriya Ovcharuk<sup>11</sup>, Alberto Viglione<sup>6</sup>, Elena Volpi<sup>12</sup>, Berit Arheimer<sup>13</sup>, Giuseppe Tito Aronica<sup>14</sup>, Ognjen Bonacci<sup>15</sup>, Ivan Čanjevac<sup>16</sup>, Andras Csik<sup>17</sup>, Natalia Frolova<sup>18</sup>, Boglarka Gmandt<sup>17</sup>, Zoltan Gribovszki<sup>19</sup>, Ali Gül<sup>20</sup>, Knut Günther<sup>21</sup>, Björn Guse<sup>21,22</sup>, Jamie Hannaford<sup>23,24</sup>, Shaun Harrigan<sup>25</sup>, Maria Kireeva<sup>18</sup>, Silvia Kohnová<sup>26</sup>, Jürgen Komma<sup>1</sup>, Jurate Kriauciuniene<sup>27</sup>, Brian Kronvang<sup>28</sup>, Deborah Lawrence<sup>29</sup>, Stefan Lüdtke<sup>21</sup>, Luis Mediero<sup>30</sup>, Bruno Merz<sup>21,31</sup>, Peter Molnar<sup>32</sup>, Conor Murphy<sup>24</sup>, Dijana Oskoruš<sup>33,34</sup>, Marzena Osuch<sup>35</sup>, Juraj Parajka<sup>1</sup>, Laurent Pfister<sup>36</sup>, Ivan Radevski<sup>37</sup>, Eric Sauquet<sup>38</sup>, Kai Schröter<sup>39</sup>, Mojca Šraj<sup>40</sup>, Jan Szolgay<sup>26</sup>, Stephen Turner<sup>23</sup>, Peter Valent<sup>1</sup>, Noora Veijalainen<sup>41</sup>, Philip J. Ward<sup>42,43</sup>, Patrick Willems<sup>44</sup>, Nenad Zivkovic<sup>45</sup>.

## Affiliations

<sup>1</sup>Institute of Hydraulic Engineering and Water Resources Management, Technische Universität Wien, Vienna, Austria.

<sup>2</sup>Czech Hydrometeorological Institute, Prague, Czechia.

<sup>3</sup>Department of Land, Environment, Agriculture and Forestry, University of Padova, Padua, Italy

<sup>4</sup>Department of Civil, Chemical, Environmental and Materials Engineering (DICAM), Università di Bologna, Bologna, Italy.

<sup>5</sup>Department of Agricultural Sciences, University of Naples Federico II, Naples, Italy.

<sup>6</sup>Department of Environment, Land and Infrastructure Engineering (DIATI), Politecnico di Torino, Turin, Italy.

<sup>7</sup>Climate Research Laboratory, Institute for Nature Management, The National Academy of Science of Belarus, Minsk, Belarus.

<sup>8</sup>Department of Hydrological Research, Ukrainian Hydrometeorological Institute, Kyiv, Ukraine.

<sup>9</sup>Department of Physical Geography and Geoecology, Faculty of Science, Charles University, Prague, Czechia.

<sup>10</sup>University of Architecture, Civil Engineering and Geodesy, Sofia, Bulgaria.

<sup>11</sup>Hydrometeorological Institute, Odessa State Environmental University, Odessa, Ukraine.

<sup>12</sup>Department of Engineering, University Roma Tre, Rome, Italy.

<sup>13</sup>Swedish Meteorological and Hydrological Institute, Norrköping, Sweden.

<sup>14</sup>Department of Engineering, University of Messina, Messina, Italy.

<sup>15</sup>Faculty of Civil Engineering, Architecture and Geodesy, Split University, Split, Croatia.

<sup>16</sup>Department of Geography, Faculty of Science, University of Zagreb, Zagreb, Croatia.

<sup>17</sup>General Directorate of Water Management, Budapest, Hungary.

<sup>18</sup>Department of Land Hydrology, Lomonosov Moscow State University, Moscow, Russia.

43 <sup>19</sup>University of Sopron, Faculty of Forestry, Institute of Geomatics and Civil Engineering, Sopron, Hungary.  
44 <sup>20</sup>Department of Civil Engineering, Faculty of Engineering, Dokuz Eylul University, Izmir, Turkey.  
45 <sup>21</sup>Helmholtz Centre Potsdam, GFZ German Research Centre for Geosciences, Section Hydrology, Potsdam,  
46 Germany.  
47 <sup>22</sup>Department of Hydrology and Water Resources Management, Institute for Natural Resource Conservation, Kiel  
48 University, Kiel, Germany  
49 <sup>23</sup>Centre for Ecology and Hydrology, Wallingford, UK.  
50 <sup>24</sup>Irish Climate Analysis and Research Units (ICARUS), Department of Geography, Maynooth University,  
51 Maynooth, Ireland.  
52 <sup>25</sup>Forecast Department, European Centre for Medium-Range Weather Forecasts (ECMWF), Reading, UK.  
53 <sup>26</sup>Department of Land and Water Resources Management, Faculty of Civil Engineering, Slovak University of  
54 Technology in Bratislava, Bratislava, Slovakia.  
55 <sup>27</sup>Lithuanian Energy Institute, Kaunas, Lithuania  
56 <sup>28</sup>Department of Ecoscience, Danish Centre for Environment and Energy, Aarhus University, Aarhus, Denmark.  
57 <sup>29</sup>Norwegian Water Resources and Energy Directorate, Oslo, Norway.  
58 <sup>30</sup>Department of Civil Engineering: Hydraulic, Energy and Environment, Universidad Politécnica de Madrid,  
59 Madrid, Spain.  
60 <sup>31</sup>Institute of Environmental Sciences and Geography, University Potsdam, Potsdam, Germany  
61 <sup>32</sup>Institute of Environmental Engineering, ETH Zurich, Zurich, Switzerland.  
62 <sup>33</sup>Department of Hydrotechnics, Faculty of Geotechnical Engineering, University of Zagreb, Varaždin, Croatia.  
63 <sup>34</sup>Croatian Meteorological and Hydrological Service, Zagreb, Croatia.  
64 <sup>35</sup>Department of Hydrology and Hydrodynamics, Institute of Geophysics Polish Academy of Sciences, Warsaw,  
65 Poland.  
66 <sup>36</sup>Luxembourg Institute of Science and Technology (LIST), Esch-sur-Alzette, Luxembourg.  
67 <sup>37</sup>Institute of Geography, Faculty of Natural Sciences and Mathematics, Ss. Cyril and Methodius University,  
68 Skopje, North Macedonia.  
69 <sup>38</sup>Irstea, UR RiverLy, Lyon-Villeurbanne, France.  
70 <sup>39</sup>Leichtweiss Institute for Hydraulic Engineering and Water Resources, Technische Universität Braunschweig,  
71 Braunschweig, Germany.  
72 <sup>40</sup>Faculty of Civil and Geodetic Engineering, University of Ljubljana, Ljubljana, Slovenia.  
73 <sup>41</sup>Finnish Environment Institute, Helsinki, Finland.  
74 <sup>42</sup>Institute for Environmental Studies (IVM), Vrije Universiteit Amsterdam, The Netherlands.  
75 <sup>43</sup>Deltares, Delft, The Netherlands.  
76 <sup>44</sup>Department of Civil Engineering, KU Leuven, Leuven, Belgium.  
77 <sup>45</sup>Faculty of Geography, University of Belgrade, Belgrade, Serbia.  
78 \*Corresponding author. E-mail: bertola@hydro.tuwien.ac.at  
79  
80

## 81 **Abstract**

82 Mega-floods that far exceed previously observed records often take citizens and  
83 experts by surprise, resulting in extremely severe damage and loss of life. Existing  
84 methods based on local and regional information rarely go beyond national borders  
85 and cannot predict these floods well because of limited data on mega-floods, and  
86 because flood generation processes of extremes differ from those of smaller, more  
87 frequently observed events. Here we analyse river discharge observations from over  
88 8000 gauging stations across Europe and show that recent mega-floods could have  
89 been anticipated from those previously observed in other places of Europe. Almost all  
90 observed mega-floods (95.5%) fall within the envelope values estimated from previous  
91 floods at other similar places on the continent, implying that local surprises are not  
92 surprising at the continental scale. This holds also for older events, indicating that  
93 mega-floods have not changed much in time relative to their spatial variability. The  
94 underlying concept of the study is that catchments with similar flood generation  
95 processes produce similar outliers. It is thus essential to transcend national  
96 boundaries and learn from other places across the continent to avoid surprises and  
97 save lives.

98

## 99 **Main Text**

100 Mega-floods that are much larger than floods experienced previously in a given  
101 catchment or region, can take citizens and local flood managers by surprise, resulting  
102 in catastrophic damage and loss of life. For example, the discharge of the July 2021  
103 flood at the Rhine tributaries in Germany, and rivers in the Netherlands, Belgium and  
104 Luxembourg, was up to four times larger than any event on record in the region<sup>1</sup>,  
105 causing almost 200 fatalities and damage in excess of \$40 billion. In this and other  
106 cases, the lack of previous local experience of events of this magnitude resulted in  
107 insufficient flood defence measures, preparedness and real-time response<sup>1,2</sup>.

108 Because of their rare occurrence, mega-floods are difficult to predict. The standard  
109 method of estimating the magnitude of potential large floods consists of fitting a  
110 probability distribution to long series of flood observations, and extrapolating the  
111 distribution to small probabilities<sup>3</sup>. However, long series that include several  
112 exceptional events are rarely available. Some estimation methods use flood  
113 observations from neighbouring catchments<sup>4</sup>, to make up for the brevity of streamflow  
114 records which, however, rarely increases the chances of capturing mega-floods. Even  
115 when such events are observed, accurate discharge estimates are difficult to obtain  
116 as the flood wave may partially bypass the gauge and difficulties with extrapolating the  
117 rating curve. Moreover, the processes that generate extreme floods tend to differ from  
118 those that generate smaller and more frequent events<sup>5</sup>, making extrapolation  
119 notoriously inaccurate. One way of capturing changing flood processes with  
120 magnitude is through rainfall-runoff models, but they require long series of precipitation  
121 and are also subject to uncertainty<sup>6,7,8</sup>. Large floods in historic or prehistoric times

122 (paleofloods) can also be used, although the information available is often not  
123 commensurate with the requirements of flood management<sup>9,10,11</sup>.

124 An alternative for enhancing the accuracy of megaflood estimates is the transfer of  
125 flood information from hydrologically similar catchments where large events may have  
126 occurred<sup>4</sup>. In Europe the occurrence of megafloods is well documented at the national  
127 scale. The August 2002 flood in Germany, Austria and Bohemia was the largest in the  
128 last half century based on economic losses; the November 1994 Piedmont flood was  
129 the second costliest event in Europe between 1970 and 2020<sup>12</sup>. Both events were  
130 caused by rainfall greater than one-third of the annual total, delivered in only 72  
131 hours<sup>13,14</sup>. However, flood information transfer rarely goes beyond national borders,  
132 and no previous study has examined megafloods in a systematic way across an entire  
133 continent, with the objective of learning from other places about the potential of future  
134 flood surprises. Some examples comparing the world's maximum measured floods  
135 also exist<sup>15</sup>, but they do not compare hydrologically similar catchments, which makes  
136 flood estimation less useful for practical purposes.

137

### 138 **Anticipating megafloods**

139 Here we analyse the most comprehensive dataset of annual maximum discharges in  
140 Europe available to date and show that recent megafloods could have been  
141 anticipated from observations in other parts of Europe, which would not be possible  
142 using national data only. We also show that the predictability of megafloods does not  
143 change in time when sub-periods are analysed. We base our analysis on annual  
144 maximum river discharge observations from 8023 gauging stations for the period  
145 1810–2021. The average length of the series is 51.4 years and the catchment areas  
146 range between 1 km<sup>2</sup> and 800,000 km<sup>2</sup>. Catchments across Europe are grouped into  
147 five hydroclimatic regions (Fig. 1) as a first step of identifying hydrologically similar  
148 catchments<sup>16</sup>. For each region, we estimate a regional envelope curve of flood  
149 discharges that represents the relationship between flood discharge and catchment  
150 area that is not exceeded by any observed flood in the region (see Methods; Extended  
151 Data Table 2). To examine possible changes in time, we also compare envelope  
152 curves obtained using observations from two 30-year sub-periods, i.e., 1961-1990 and  
153 1991-2020.

154 We focus on 498 catchments (“target” catchments) where 510 recent (i.e. after 1999)  
155 megafloods that are surprising based on local data are identified (see Methods). To  
156 evaluate the possibility of anticipating megafloods in target catchments using  
157 information from other places in Europe, we perform a hindcast experiment of  
158 predicting their peak discharge with regional envelope curves, using flood  
159 observations from similar catchments up to the year before their occurrence. For each  
160 target catchment, a group of similar catchments (“donor” catchments) is identified in  
161 the corresponding hydroclimatic region based on the similarity of catchment area and  
162 the mean and coefficient of variation of the truncated flood series (up to the year before  
163 the megaflood). From this group of donor catchments we construct an envelope curve

164 which we compare with the megaflood that occurred later in the target catchments.  
165 We repeat this analysis for all 510 detected megafloods in the target catchments.

166

### 167 **European envelope curves of flood discharges**

168 Our data show that recent megafloods have occurred in all regions of Europe, although  
169 they are more frequent in the Atlantic and Continental regions (Fig.1; Extended Data  
170 Table 3), where respectively 8.7% and 7.2% of the catchments exhibit recent  
171 megafloods. In the Boreal region, the respective value is only 1.3%. The smaller value  
172 is related to the smaller interannual variability of floods in the Boreal region<sup>17</sup>.

173 In the Atlantic region, the megafloods (coloured points in Fig. 1b-f) are on average 3.4  
174 times larger than the local mean annual maximum discharges (squares), while in the  
175 Continental and Mediterranean regions they are 5.3 and 5.2 times larger (Extended  
176 Data Table 3). The larger ratio in the Mediterranean is likely related to the more non-  
177 linear rainfall-runoff process and more variable precipitation in arid than in humid  
178 climates<sup>5,18</sup>. However this analysis is not able to conclude whether megafloods are  
179 becoming more frequent or not.

180 The envelope curves defined by the largest floods also differ between hydroclimatic  
181 regions in terms of their intercept and slope (thick continuous lines in Fig. 1b-f;  
182 Extended Data Table 2). For a catchment size of 1000 km<sup>2</sup>, the envelope specific  
183 discharge in the Mediterranean region is 5.26 m<sup>3</sup>s<sup>-1</sup>km<sup>-2</sup> while in the Boreal region it is  
184 1.37 m<sup>3</sup>s<sup>-1</sup>km<sup>-2</sup>. This is because the flood-inducing rainstorms in the Mediterranean  
185 are associated with much larger intensities than the flood-inducing snowmelt typical of  
186 Northern Europe. The slopes of the envelope curves are steepest in the Mediterranean  
187 area (-0.57) and flattest (-0.07) in the Boreal region (Fig. 1). This is because the  
188 Mediterranean rainstorms tend to be more localised than the snowmelt in the North of  
189 Europe. The envelope curves for the most recent sub-period (thin dotted lines) tend to  
190 be slightly lower than those for the first sub-period (thin dashed lines), except for the  
191 Mediterranean and the Atlantic region. The median regression curves (thin continuous  
192 lines) are slightly flatter than the respective envelopes, as larger catchments tend to  
193 have more regular flood regimes than small ones. Figs. 1g-j illustrate examples of flood  
194 series in pairs of catchments with and without megafloods.

195 To illustrate the potential of anticipating megafloods from other places in Europe, Fig.  
196 2 shows three examples. The 2002 flood in the Kamp catchment in Austria (Fig. 2a)  
197 peaked at 459 m<sup>3</sup>s<sup>-1</sup> which is equivalent to a specific discharge of 0.74 m<sup>3</sup>s<sup>-1</sup>km<sup>-2</sup> (black  
198 triangle) given the catchment area of 622 km<sup>2</sup>. The envelope curve (blue line), defined  
199 by the hydrologically similar catchments within the hydroclimatic region, gives a  
200 specific discharge of 1.68 m<sup>3</sup>s<sup>-1</sup>km<sup>-2</sup>. This means that, in light of European floods, the  
201 Kamp was not at all surprising while for the locals it was<sup>19</sup>. The regional envelope  
202 discharge illustrated in Fig. 2 is defined based on previously observed floods in various  
203 European countries, including Bulgaria and Poland (blue circles in Fig. 2d).

204 The 2009 flood in the Cumbrian Derwent catchment in the UK (Fig. 2b) peaked at 0.84  
205  $\text{m}^3\text{s}^{-1}\text{km}^{-2}$  and was 58% larger than the second largest event on record which occurred  
206 in 2005. The corresponding envelope specific discharge is  $1.64 \text{ m}^3\text{s}^{-1}\text{km}^{-2}$ . Much larger  
207 extremes were observed in similar catchments in Norway (Fig. 2e). The 2009  
208 megaflood in the Derwent was itself exceeded in 2015, however this later event still  
209 lies below the envelope curve and was not as surprising as the 2009 event (11%  
210 larger)<sup>2</sup>.

211 The 2021 flood in the Ahr catchment in Germany (Fig. 2c) peaked at  $0.80 \text{ m}^3\text{s}^{-1}\text{km}^{-2}$ ,  
212 similar to the Kamp flood, with an envelope estimate of  $1.57 \text{ m}^3\text{s}^{-1}\text{km}^{-2}$ . For the Ahr  
213 catchment, the similar catchments making up the donor group are, in descending order  
214 of flood magnitude: the Timis in Romania, the Freiburger Mulde in Germany, the  
215 Maritsa in Bulgaria, the Ljig in Serbia, the Lausitzer Neisse in Germany, the Corrèze  
216 and Le Lot in France, the Nysa Kłodzka in Poland and the Birs in Switzerland (Fig. 3).  
217 Although each of these catchments has a specific hydrological behaviour, overall they  
218 can be considered hydrologically similar to the Ahr in terms of average climate and  
219 flood statistical properties. All of these ten catchments experienced record-breaking  
220 floods that were surprising based on previously observed events at that location, and  
221 these occurred in the period before 2021 (Fig. 3).

222 The analysis of Fig. 2 is repeated for all 510 recent megafloods in the target  
223 catchments in Europe (Fig. 4). In 95.5% of the target catchments, the discharge of the  
224 envelope is larger than that of the observed megaflood, suggesting that, from a  
225 European perspective, almost none of the events can be considered a regional  
226 surprise. In 9.6% of the cases, the observed megafloods are within 75% and 150% of  
227 the envelope (red points in Fig. 4a), i.e. the order of magnitude is similar. The target  
228 catchments are distributed all over Europe with a higher concentration in the West  
229 (Fig. 4b), reflecting positive trends in flood magnitudes in Western Europe<sup>20,21</sup> and, to  
230 some degree, the higher station density.

231 The prediction is also conducted for 151 and 188 catchments with 151 and 190 recent  
232 (i.e. in the last 10 years of each sub-period) megafloods in the first and second sub-  
233 period, respectively. The distribution of the ratio between observed and predicted  
234 discharge (inset of Fig. 4a) indicates that there are no substantial changes in the  
235 predictability of megafloods in time. The discharge of the envelope is larger than that  
236 of the observed megaflood in 92% and 93.7% of the respective target catchments.

237 To evaluate the suitability of the donor selection, we compare the timing within the  
238 year of the target megafloods with that of the ten largest floods in the donor catchments  
239 (Fig. 4c). Flood timing is a proxy of flood generation processes<sup>22</sup>. Fig. 4c shows that  
240 the timing of the target megafloods (black lines) generally agrees with that of the  
241 donors (brown lines), both in terms of the average timing (angle from the centre of the  
242 circle) and the consistency of timing between events (distance to the centre). The  
243 agreement points towards the plausibility of the donor selection and prediction. A  
244 tendency for the observed timings to be more bimodal than the predictions is likely  
245 related to the smaller number of events.

246

## 247 **Implications of expanding the perspective**

248 Whereas previous studies have assessed the potential for megafloods mainly based  
249 on local or regional data, this study expands the observation area to the continental  
250 scale. We use megafloods that have occurred in hydrologically similar catchments  
251 elsewhere on the continent as a surrogate for the megafloods that could happen in the  
252 catchment of interest in the future.

253 The degree to which this transfer of information is possible depends on the suitable  
254 choice of donor catchments based on the notion of hydrological similarity<sup>23</sup>. The  
255 underlying concept is that catchments with similar flood generation processes,  
256 including rainfall, infiltration and flow paths, produce similar outliers, as these  
257 processes determine the transition from smaller to larger events<sup>5,24,25</sup>. Here we use  
258 catchment area and the mean and coefficient of variation of the truncated flood series  
259 within the same hydroclimatic region as a proxy of similarity in flood generation  
260 processes. While other similarity measures exist<sup>16</sup>, our donor catchment selection is  
261 deemed plausible because of the similarity of the timing within the year of the events,  
262 given that timing is a fingerprint of the interplay between climatic and catchment  
263 processes<sup>22</sup>. Additional spot testing of catchment pairs (such as the Ahr catchment in  
264 Germany paired with the Timis catchment in Romania) based on prior knowledge from  
265 the literature<sup>1,25</sup> confirms the similarity. To assess robustness of the method we  
266 conduct a sensitivity analysis on the parameters of the similarity criteria and the choice  
267 of hydroclimatic regions (Extended Data Fig. 1-8). The results show that changing  
268 parameters and/or regions may modify individual donor catchments, but the envelope  
269 curve that arises from the set of donor catchments is affected much less (see method  
270 section for details).

271 The cross-validation experiment conducted here, starting from observed megafloods,  
272 withholding them and only using data from floods that have occurred previously,  
273 mimics the case of anticipating megafloods that have not yet occurred. We show that  
274 it is indeed feasible to estimate the order of magnitude of possible future megafloods.  
275 Almost all observed megafloods (95.5%) are smaller than the envelope values  
276 estimated, i.e. the local surprises are not surprising at the continental scale. Similar  
277 results are found for different sub-periods, indicating that megafloods have not  
278 changed much in time relative to their spatial variability within Europe. These findings  
279 are in line with recent studies in the US showing little evidence for temporal trends of  
280 large floods<sup>26</sup>.

281 The proposed envelope curve approach complements alternative methods such as  
282 regional statistical approaches that spatially interpolate observed discharges<sup>4</sup> or  
283 process-based rainfall-runoff modelling<sup>27</sup>. These methods provide best estimates of  
284 expected floods, while the envelope method reflects a possible worst case – which  
285 itself is an important aspect of flood risk planning.



286 The focus on a possible worst case implies that the envelope values are generally too  
287 large to serve as design values for most types of flood defence infrastructure from a  
288 cost-benefit perspective. Rather, they describe a possibility space<sup>28</sup> that is prudent to  
289 consider as civil protection scenarios, required to organise local preparedness, and  
290 for testing the safety of very large dams. They can be used to derive extreme flood  
291 hazard scenarios, either failure scenarios (what can go wrong?) or future development  
292 scenarios (what could the future look like?) that could strengthen existing methods  
293 such as the Probable Maximum Flood (PMF) concept<sup>29</sup>. There is an increasing need  
294 for considering the extremes of the extremes, as there is a tendency in society for  
295 smaller acceptable risks<sup>29</sup>, so flood risk management should account for the potential  
296 of surprises and their devastating consequences. This requires a shift in thinking<sup>29</sup> and  
297 the application of envelope curves, storylines<sup>2,30</sup> and compound event analyses<sup>31</sup>.  
298 Making individuals and societies more robust against surprises therefore goes beyond  
299 the design of spillways and flood management plans.

300 In summary, to anticipate megafloods we must learn from other places in order to  
301 reduce the surprise factor of their occurrence, increase flood risk awareness and  
302 enhance preparedness of flood risk management. To this end, it is essential to move  
303 beyond national flood risk assessment and share information on megafloods across  
304 countries and continents.

305

## 306 **Acknowledgements**

307 We acknowledge all flood data providers listed in Extended Data Table 1. G. Blöschl and M. Bertola  
308 were supported by the FWF projects 'SPATE' (I 3174, I 4776) and W1219-N22. B. Merz and B.  
309 Guse were supported by the DFG 'SPATE' project (FOR 2416). A. Viglione, P. Claps, D. Ganora,  
310 M. Borga and E. Dallan were supported by the European Union Next-GenerationEU 'RETURN'  
311 Extended Partnership (National Recovery and Resilience Plan – NRRP, Mission 4, Component  
312 2, Investment 1.3 – D.D. 1243 2/8/2022, PE0000005). S. Kohnová and J. Szolgay were supported  
313 by the Slovak Research and Development Agency (number APVV-20-0374) and the VEGA Grant  
314 Agency (number 1/0782/21). J. Hannaford and S. Turner were supported by the ROBIN (Reference  
315 Observatory of Basins for INternational hydrological climate change detection) initiative, with  
316 funding from the Natural Environment Research Council (grant number NE/W004038/1). The  
317 authors acknowledge the involvement in the data screening process of M. Haas.

318

## 319 **Author Contributions Statement**

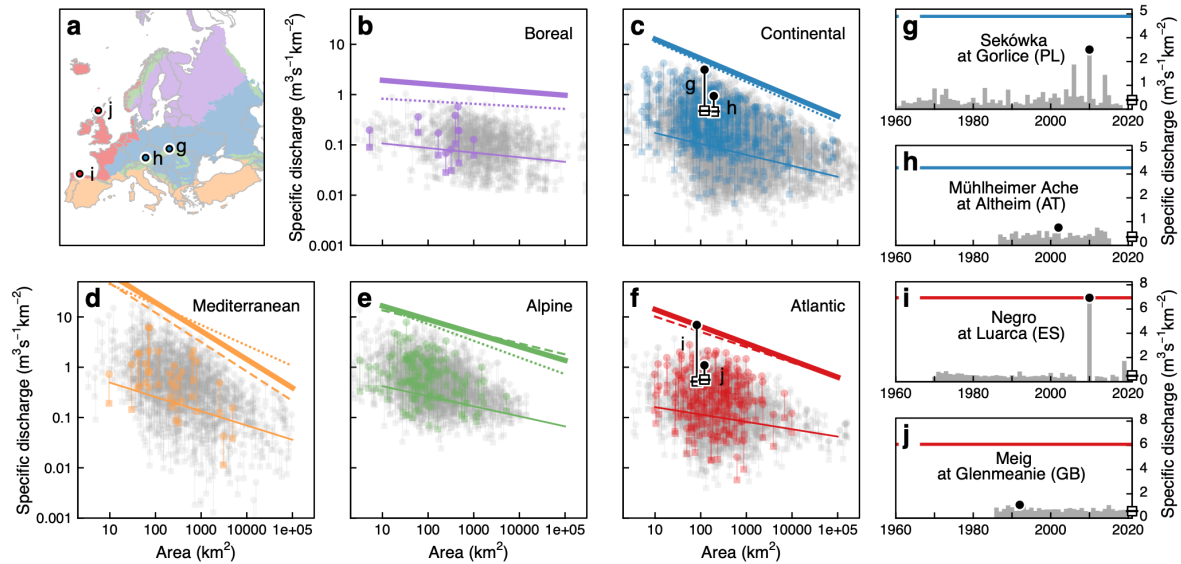
320 G. Blöschl and M. Bertola initiated the study and wrote the first draft of the paper. M. Bertola, G.  
321 Blöschl, M. Borga, A.C., P.C., E.D., D.G., A.M., A.V. and E.V. designed the study. M. Bertola  
322 collated the updated version of the database with the help of most of the co-authors and conducted  
323 the analyses. G. Blöschl, M. Bertola, interpreted the results in the context of underlying geophysical  
324 mechanisms. G. Boglarka, M. Boháč, A.C., S.K., O.L., S.L. M.M.-G., K.G., Z.G., B.G., J.K., B.M.,  
325 P.M., J.P., L.P., I.R., K.S., J.S., P.V., P. Ward, P. Willems., and N.Ž. interpreted the results in  
326 central Europe. G.T.A., O.B., M. Borga, A.C., I.Č., G.B.C., P.C., E.D., D.G., A.G., A.M., L.M., D.O.,  
327 M.Š., A.V. and E.V. interpreted the results in southern Europe. B.A., B.K., D.L., and N.V.  
328 interpreted the results in northern Europe. J.H., S.H., C.M., S.T., and E.S. interpreted the results  
329 in western Europe. I.D., N.F., L.G., M.K., J.K., M.O. and V.O. interpreted the results in eastern  
330 Europe. All authors contributed to framing and revising the paper.

331  
332

### 333 Competing Interests Statement

334 The authors declare no competing interests.  
335

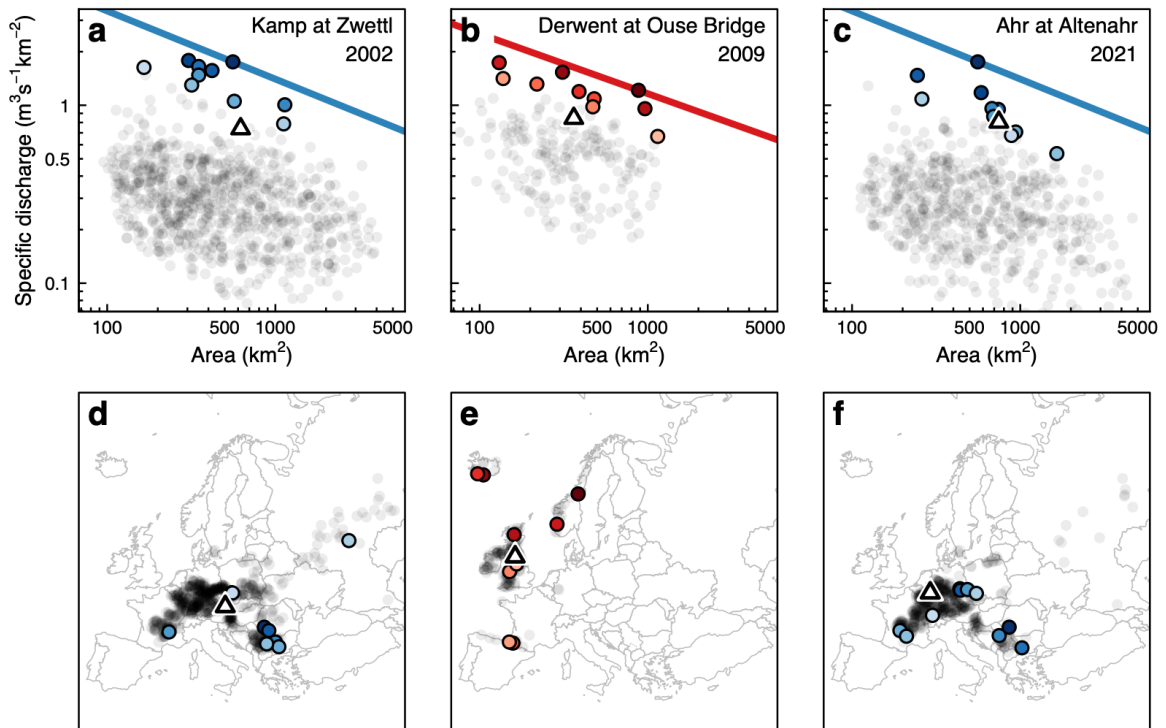
### 336 Figure Captions



337

338 **Fig. 1: Megafoods in Europe.** (a) Five hydroclimatic regions: Boreal (purple),  
339 Continental (blue), Mediterranean (orange), Alpine (green) and Atlantic (red). (b-f)  
340 Maximum observed specific flood discharges (points) and mean of annual specific  
341 flood discharges (squares) over the entire observation period at each stream gauge  
342 as a function of catchment area. Regional envelope curves (thick lines) and median  
343 regional annual specific flood discharges (thin lines) for the full record period are  
344 shown for each hydroclimatic region. Envelope curves for two 30-year sub-periods are  
345 also shown (dashed lines for 1961-1990, dotted lines for 1991-2020). Parameters of  
346 the envelope curves are listed in Extended Data Table 2. Coloured symbols indicate  
347 the mean and maximum flood discharges in the 498 catchments with recent  
348 megafoods, grey points those of the remaining catchments. (g-j) Examples of series  
349 of annual flood discharges with (g and i) and without (h and j) megafoods; their  
350 corresponding mean (squares) and maximum values (points) are highlighted in black  
351 in (c) and (f). The locations of corresponding stream gauges are indicated in (a) by  
352 circles.

353



354

355 **Fig. 2: Envelope curves for three catchments with recent megafloods in Europe.**

356 (a,d) Kamp (622 km<sup>2</sup> catchment area) with 2002 flood; (b,e) Cumbrian Derwent (363

357 km<sup>2</sup>) with 2009 flood, and (c,f) Ahr (746 km<sup>2</sup>) with 2021 flood, indicated with triangles.

358 (a-c) Maximum specific discharges observed before the year of occurrence of the

359 megaflood for 824 (a), 196 (b) and 590 (c) similar donor catchments (points) selected

360 within the corresponding hydroclimatic region. Coloured points indicate ten largest

361 events (in terms of distance to the envelope curve), with shades being darker for

362 events that are closer to the envelope.

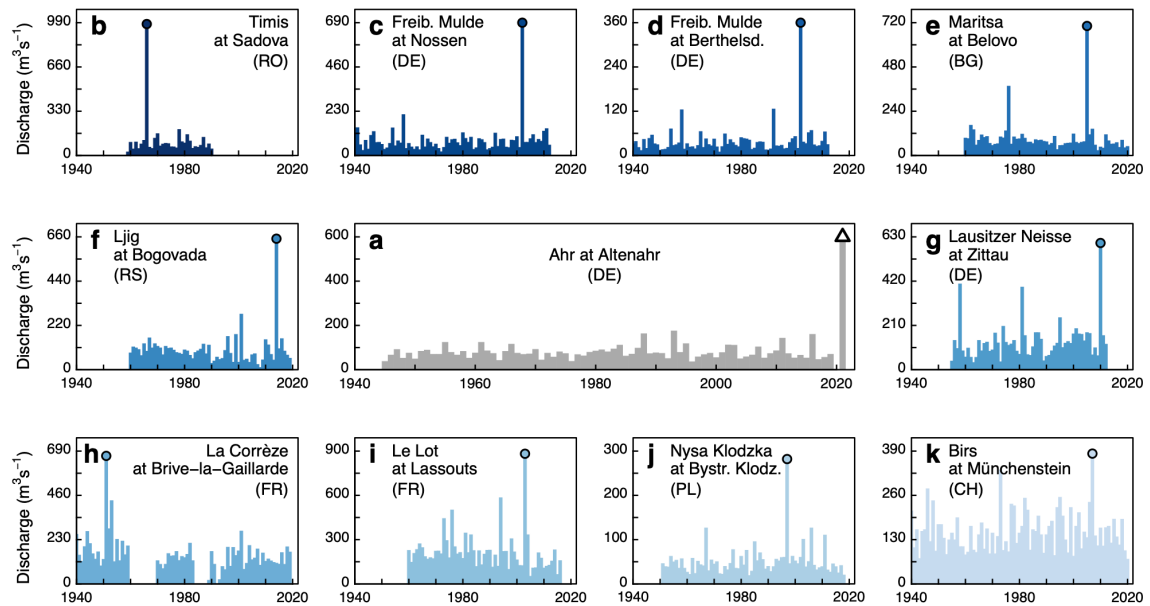
363 Line shows resulting envelope curve with the slope estimated from the hydroclimatic regions (Fig. 1b-f).

364 (d-f) Location of the target (triangle) and donor (points) catchments. Note that the envelope curves of Fig. 1 refer

365 to the entire hydroclimatic region, while here they refer to the donor group within a

366 region.

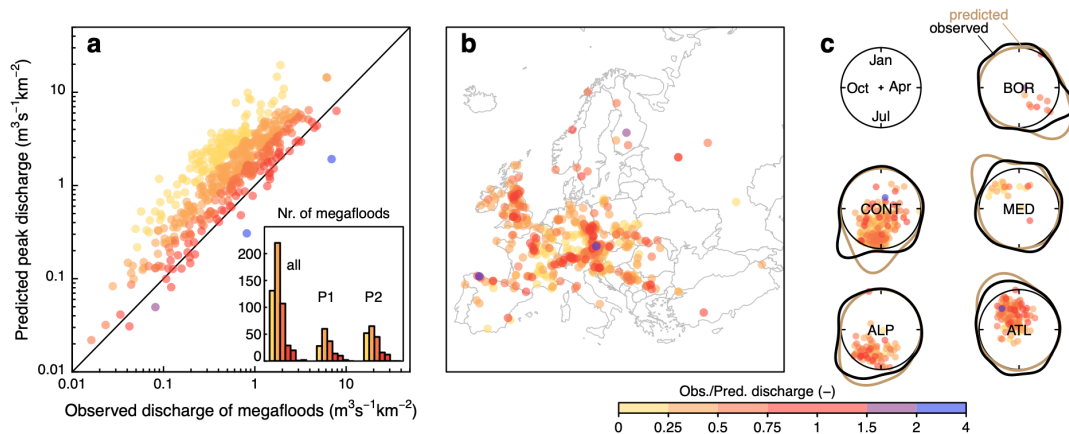
367



368

369 **Fig. 3: Annual flood series for the Ahr and ten donor catchments with extreme**  
 370 **floods.** (a) Ahr at Altenahr, Germany, with 2021 mega-flood (the target event) indicated  
 371 as a triangle. (b-k) Series for the ten donor catchments indicates as coloured dots in  
 372 Fig. 2c,f).

373



374

375 **Fig. 4: Predicted versus observed mega-floods.** (a) Predicted specific envelope  
 376 discharge for 498 target catchments versus observed specific discharge of the  
 377 mega-floods in the same catchments. Predicted envelope discharges are estimated  
 378 using discharge observations from a pool of donor catchments up to the year before  
 379 the target mega-flood. The number of target mega-floods is shown in the inset for the  
 380 entire period ("all") and the two sub-periods 1961-1990 ("P1") and 1991-2020 ("P2").  
 381 Colours indicate the ratio of observed and predicted discharge. (b) Location of target  
 382 catchments. Mega-floods occur all over Europe and are less surprising than commonly  
 383 assumed. (c) Circular distribution of the timing of the mega-floods observed in the

384 target catchments (black lines), and mean timing of the 10 largest floods in the donor  
385 catchments (coloured points) and their distribution (brown lines). The distance of the  
386 points to the centre is inversely proportional to the standard deviation of the flood  
387 timing.

388  
389

## 390 **References**

- 391 1. Apel, H., Vorogushyn, S., & Merz, B. Brief communication—Impact Forecasting Could  
392 Substantially Improve the Emergency Management of Deadly Floods: Case Study July 2021  
393 floods in Germany. *Natural Hazards and Earth System Sciences Discussions*, 1-10 (2022).
- 394 2. Kreibich, H., Van Loon, A.F., Schröter, K. et al. The challenge of unprecedented floods and  
395 droughts in risk management. *Nature* 608, 80–86 (2022).
- 396 3. De Niel, J., Demarée, G., Willems, P. Weather typing based flood frequency analysis validated for  
397 exceptional historical events of past 500 years along the Meuse river, *Water Resources*  
398 *Research*, 53(10), 8459-8474 (2017).
- 399 4. Robson, A. J. and Reed, D. W. Flood Estimation Handbook (FEH), chap. Statistical procedures  
400 for flood frequency estimation, p. Vol. 3, Institute of Hydrology, Wallingford, UK (1999).
- 401 5. Rogger, M., Pirkl, H., Viglione, A., Komma, J., Kohl, B., Kirnbauer, R., Merz, R., & Blöschl, G.  
402 (2012). Step changes in the flood frequency curve: Process controls. *Water Resources Research*,  
403 48(5), 1–15.
- 404 6. Bergstrand M., Asp S. and Lindström G. Nationwide hydrological statistics for Sweden with high  
405 resolution using the hydrological model S-HYPE. *Hydrology Research*, 45.3, 349-356 (2014).
- 406 7. Devitt, L., Neal, J., Wagener, T., & Coxon, G. Uncertainty in the extreme flood magnitude  
407 estimates of large-scale flood hazard models. *Environmental Research Letters*, 16(6), 064013  
408 (2021).
- 409 8. Bouaziz, L. et al. Behind the scenes of streamflow model performance, *Hydrol. Earth Syst. Sci.*,  
410 25, 1069–1095 (2021).
- 411 9. Kjeldsen, T.R. et al. Documentary evidence of past floods in Europe and their utility in flood  
412 frequency estimation. *Journal of Hydrology*, 517, 963–973 (2014).
- 413 10. Blöschl, G., Kiss, A., Viglione et al. Current European flood-rich period exceptional compared with  
414 past 500 years. *Nature*, 583(7817), 560–566 (2020).
- 415 11. U.S. Geological Survey Scientific Investigations Report 2020–5065, 89 p. (2020).
- 416 12. World Meteorological Organisation (WMO). WMO Atlas of Mortality and Economic Losses from  
417 Weather, Climate and Water Extremes (1970–2019). WMO-No. 1267 (2021).
- 418 13. Blöschl, G., Nester, T., Komma, J., Parajka, J., & Perdigão, R. A. P. The June 2013 flood in the  
419 Upper Danube Basin, and comparisons with the 2002, 1954 and 1899 floods. *Hydrology and*  
420 *Earth System Sciences*, 17(12), 5197–5212 (2013).
- 421 14. Lionetti, M. The Italian floods of 4–6 November 1994. *Weather*, 51(1), 18-27 (1996).
- 422 15. Herschy, R. W. (2002). The world's maximum observed floods. *Flow Measurement and*  
423 *Instrumentation*, 13(5–6), 231–235. [https://doi.org/10.1016/S0955-5986\(02\)00054-7](https://doi.org/10.1016/S0955-5986(02)00054-7)
- 424 16. Kuentz, A., Arheimer, B., Hundecha, Y., and Wagener, T. Understanding hydrologic variability  
425 across Europe through catchment classification, *Hydrol. Earth Syst. Sci.*, 21, 2863-2879 (2017)

- 426 17. Lun, D., Viglione, A., Bertola, M., Komma, J., Parajka, J., Valent, P., & Blöschl, G. Characteristics  
427 and process controls of statistical flood moments in Europe – a data-based analysis. *Hydrology*  
428 and *Earth System Sciences*, 25(10), 5535–5560 (2021).
- 429 18. Blöschl, G. Flood generation: process patterns from the raindrop to the ocean, *Hydrol. Earth Syst.*  
430 *Sci.*, 26, 2469–2480 (2022)
- 431 19. Blöschl, G. Flood warning - on the value of local information. *International Journal of River Basin*  
432 *Management*, 6 (1), pp. 41-50 (2008).
- 433 20. Blöschl, G., Hall, J., Viglione, A. et al. Changing climate both increases and decreases European  
434 river floods. *Nature*, 573(7772), 108–111 (2019).
- 435 21. Bertola, M., Viglione, A., Lun, D., Hall, J., & Blöschl, G. Flood trends in Europe: are changes in  
436 small and big floods different? *Hydrology and Earth System Sciences*, 24(4), 1805–1822 (2020).
- 437 22. Blöschl, G., Hall, J., Parajka, J., Perdigão, R. A., Merz, B., Arheimer, B., ... & Živkoviæ, N.  
438 Changing climate shifts timing of European floods. *Science*, 357(6351), 588-590 (2017).
- 439 23. Blöschl, G., Sivapalan, M., Wagener, T., Viglione, A., Savenije, H.H. *Runoff Prediction in*  
440 *Ungauged Basins – Synthesis across Processes, Places and Scales*. Cambridge University Press  
441 (2013).
- 442 24. Kemter, M., Merz, B., Marwan, N., Vorogushyn, S., & Blöschl, G. Joint Trends in Flood  
443 Magnitudes and Spatial Extents Across Europe. *Geophysical Research Letters*, 47(7), 1–8  
444 (2020).
- 445 25. Popescu, I., Jonoski, A., Van Andel, S. J., Onyari, E., & Moya Quiroga, V. G. Integrated modelling  
446 for flood risk mitigation in Romania: case study of the Timis–Bega river basin. *International journal*  
447 *of river basin management*, 8(3-4), 269-280 (2010).
- 448 26. Collins, M. J., Hodgkins, G. A., Archfield, S. A., & Hirsch, R. M. (2022). The occurrence of large  
449 floods in the United States in the modern hydroclimate regime: Seasonality, trends, and large-  
450 scale climate associations. *Water Resources Research*, 58,  
451 e2021WR030480. <https://doi.org/10.1029/2021WR030480>
- 452 27. Donnelly, C, Andersson, J.C.M. and Arheimer, B. Using flow signatures and catchment similarities  
453 to evaluate a multi-basin model (E-HYPE) across Europe. *Hydr. Sciences Journal* 61(2):255-273  
454 (2016)
- 455 28. Sivapalan, M., & Blöschl, G. Time scale interactions and the coevolution of humans and water.  
456 *Water Resources Research*, 51(9), 6988–7022 (2015).
- 457 29. Merz, B., Vorogushyn, S., Lall, U., Viglione, A., & Blöschl, G. Charting unknown waters-On the  
458 role of surprise in flood risk assessment and management. *Water Resources Research*, 51(8),  
459 6399–6416 (2015).
- 460 30. Shepherd, T. G. Storyline approach to the construction of regional climate change information.  
461 *Proceedings of the Royal Society A*, 475(2225), 20190013 (2019).
- 462 31. Thieken, A. H., Samprogna Mohor, G., Kreibich, H., and Müller, M.: Compound inland flood  
463 events: different pathways, different impacts and different coping options, *Nat. Hazards Earth*  
464 *Syst. Sci.*, 22, 165–185 (2022).

465

## 466 **Methods**

467

### 468 **Datasets**

469 The hydrological data used in this study were obtained from a pan-European Flood  
470 Database<sup>32</sup> with subsequent updates. The current version contains data from 8,023  
471 hydrometric gauging stations from 68 European data sources for the period 1810–  
472 2021 (Extended Data Table 1). The dataset consists of the highest discharge (daily  
473 mean or instantaneous discharge) in each calendar year for each station. The stations  
474 are located within the domain bounded by 22.25° W–63.25° E and 34.25° N–71.25° N  
475 (Extended Data Fig. 1), and catchment areas range between 1 km<sup>2</sup> and 800,000 km<sup>2</sup>.  
476 The dataset was screened for data errors. The screening involved visual examination  
477 of the flood records, analysis of flood seasonality and examination of the gauge  
478 location and catchment area in Google Maps. All available stations, including those  
479 affected by reservoir construction, were considered for the analysis because reservoir  
480 effects were deemed to have little significance for envelope curves for large  
481 hydroclimatic regions. Similarly, all available years with data were considered  
482 notwithstanding differences in the record lengths, because the focus was on the  
483 maxima observations of each series. The minimum series length is 10 years, and the  
484 average length is 51.4 years.

485 The gauging stations were grouped into five regions (Fig. 1a; Extended Data Fig.1)  
486 that reflect similar hydroclimatic conditions by generalising the European  
487 Biogeographical regions<sup>33</sup> with a view on flood processes. The Steppic and Pannonian  
488 regions were merged with the Continental region, the Arctic region with the Boreal  
489 region, and the Anatolian and Black Sea regions with the Mediterranean region.  
490 Additionally, part of northern Italy was considered as part of the Mediterranean region  
491 and Iceland as part of the Atlantic region. For comparison, an alternative subdivision  
492 of Europe into five regions<sup>17</sup> was considered in a sensitivity analysis (Extended Data  
493 Fig. 4a). In order to examine possible changes, the observation period was subdivided  
494 into two 30-year sub-periods, P1 (1961-1990) and P2 (1991-2020).

495

### 496 **Regional envelope curves**

497 We quantified the largest flood events in each region by scaling the peak discharges  
498 by catchment area via envelope curves that represent the upper limit of the dataset  
499 (Fig. 1):

$$500 \quad \log(q) = a + b \cdot \log(A) \quad (1)$$

501 where  $q$  (m<sup>3</sup>s<sup>-1</sup>km<sup>-2</sup>) is the specific discharge, i.e. the discharge per unit catchment  
502 area  $A$ . The parameter  $b$  was estimated by quantile regression with quantile  $z=0.999$   
503 using the `rq` function of the R `quantreg` package<sup>34,35</sup>. The quantile regression enables  
504 a more robust estimate than the tangents on the maxima, because it uses the complete  
505 dataset rather than the maxima only. The intercept  $a$  was determined such that it

506 satisfies the envelope condition, i.e. the envelope curve is the upper bound of all  
 507 observed flood discharges in a region (Extended Data Table 2). For comparison, a  
 508 quantile regression with  $z=0.5$  is also shown in Fig. 1 (thin line).  
 509

## 510 **Megafloods**

511 For the selection of recent megafloods (Fig. 4) the following criteria were adopted:  
 512 (i) the discharge value is a high outlier in the corresponding series of annual maximum  
 513 flood discharges, according to the definition<sup>36</sup>:

$$514 \quad q_{mf} > Q_3 + k * (Q_3 - Q_1) \quad (2)$$

515 where  $Q_1$  and  $Q_3$  are the first and third quartile (i.e. respectively 25% and 75% of the  
 516 observations lies below this values) and  $k=3$ ;

517 (ii) the discharge value is record-breaking and locally surprising, i.e., its return period  
 518  $T_{mf}$  is at least 3 times larger than the return period of the second largest event up to  
 519 that year  $T_{sl}$ . The return period was obtained by fitting a GEV distribution to each flood  
 520 series up to the year of the megaflood using the L-moments (R extRemes package).

521 (iii) it occurred after the year 1999 (when the full observation period is analysed) and  
 522 the corresponding series has at least 20 years of data previous to the event.

523 The selection resulted in a set of 510 megafloods from 498 target catchments, whose  
 524 observed specific discharge and location of corresponding gauges are shown in Fig.  
 525 4a and 4b. When detecting megafloods in the two 30-year sub-periods, only  
 526 observations within each sub-period are considered and the criterion (iii) is modified  
 527 such that events in the last 10 years of the respective sub-period are selected (i.e.  
 528 after 1979 for P1 and after 2009 for P2).

529 We tested the robustness of the results to the criterion (i) for the selection of high  
 530 outliers, using the definition for skewed data<sup>37</sup>:

$$531 \quad \begin{cases} q_{mf} > Q_3 + 1.5e^{3MC} IQR & \text{if } MC > 0 \\ q_{mf} > Q_3 + 1.5e^{4MC} IQR & \text{if } MC < 0 \end{cases} \quad (3)$$

532 Where MC is the medcouple<sup>38</sup>, a robust measure of skewness, defined as:

$$533 \quad MC(X_n) = \text{med}_{x_i \leq m_n \leq x_j} h(x_i, x_j) \quad (4)$$

534 with  $m_n$  is the sample median of  $X_n$  and

$$535 \quad h(x_i, x_j) = \frac{(x_j - m_n) - (m_n - x_i)}{x_j - x_i} \quad (5)$$

536 The alternative selection resulted in a set of 677 megafloods (Supplementary Fig. S1),  
 537 whose observed specific discharge and location of corresponding gauges are shown  
 538 in Supplementary Fig. S2.



539 We also tested the sensitivity of the results to criterion (ii) for the selection of record-  
 540 breaking and surprising events, by varying the threshold  $T_{mf}/T_{sl}$  between 1 and 4. The  
 541 results of the sensitivity analysis are shown in Supplementary Fig. S3 and indicate  
 542 that, when the definition of megafloods is extended to less surprising events (i.e.  $T_{mf}/T_{sl}$   
 543  $<3$ ), the fraction of megafloods larger than the envelope is unchanged. The only  
 544 exception is the Boreal region, where fewer events are selected.

545

## 546 Donor catchments

547 For each catchment in which a megaflood had occurred (target catchment), a pool of  
 548 similar catchments (donor catchments) was identified in the same region. The  
 549 similarity between the catchments was quantified in terms of weighted normalised  
 550 Euclidean distance  $D$  in a three-dimensional space with the following dimensions: the  
 551 logarithm of catchment area  $A$ , the logarithm of the mean of the annual maximum  
 552 specific discharges  $q_m$  normalised to a catchment area of 100km<sup>2</sup>, and the coefficient  
 553 of variation  $CV$  of the annual maximum discharges:

$$554 \quad D = \sqrt{\alpha \left( \frac{\log A_i - \log A_j}{sd(\log A)} \right)^2 + \beta \left( \frac{\log q_{m,i} - \log q_{m,j}}{sd(\log q_m)} \right)^2 + \gamma \left( \frac{CV_i - CV_j}{sd(CV)} \right)^2} \quad (6)$$

555 where  $i$  refers to the target catchment,  $j$  to a potential donor catchment and  $sd$  is the  
 556 standard deviation of all catchments in the donor group. Greek letters indicate weights.  
 557  $q_m$  and  $CV$  were calculated on flood data prior to the year of occurrence of the target  
 558 event to obtain a cross-validation experiment that resembles a case of anticipating  
 559 megafloods a priori. In estimating  $q_m$  and  $CV$  we excluded outliers (for both the target  
 560 and the donor catchments) according to the criterion of Eq. (2), because megafloods  
 561 should not influence the comparison, and only smaller, frequently occurring floods  
 562 were used, which is the only information usually available in the case of a prediction.  
 563 In selecting the number of catchments in the pooling group, there is a tradeoff between  
 564 a larger group that has a higher chance of containing very large floods, and a smaller  
 565 group that is hydrologically more homogeneous. For Fig. 1, 2, 3 we used  $\alpha=\beta=\gamma=1$   
 566 (corresponding to the assumption of the three dimensions having the same  
 567 importance) and included catchments with  $D < D_{max}$  with  $D_{max}=1$ , guided by a sensitivity  
 568 analysis (see below and Extended Data Fig. 2).

569

## 570 Megaflood prediction

571 We repeated the selection of the donor group for each target catchment and estimated  
 572 the envelope curve, using the slope  $b$  of the corresponding hydroclimatic region and  
 573 the intercept determined as the minimum that satisfies the envelope condition of the  
 574 group only. The procedure only uses observations from donor catchments up to the  
 575 year before the megaflood in the target catchment (Fig. 2a-c). We finally obtained an  
 576 estimate of the discharge of a potential megaflood in the target catchment (predicted

577 megaflood) from the envelope curve and compared it to the discharge of the observed  
578 megaflood (Fig. 4a).

579 In order to evaluate the plausibility of the donor selection we analysed the timing of  
580 the megafloods observed in the target and donor catchments using previously  
581 established methods<sup>22</sup> (Fig. 4c). We compared the distribution of the timing of the  
582 observed megafloods to the average timing of the 10 largest floods in the donor group.  
583 The circular distributions in Fig. 4c were obtained using the R circular package.

584

585 In order to evaluate the robustness of the method we conducted a number of sensitivity  
586 analyses. We varied  $D_{max}$  between 0.5 and 1.5 and showed that an increase in  $D_{max}$   
587 translates into an increasing number of target megafloods that are below the envelope  
588 (Extended Data Fig. 2). The larger fraction in the Boreal region is because of fewer  
589 donors available compared to the other regions. We also tested the sensitivity of  $\alpha$ ,  $\beta$   
590 and  $\gamma$ , examining four weight combinations: equal weights ( $\alpha=\beta=\gamma=1$ ) and doubling  
591 one of the weights ( $\alpha=2$  and  $\beta=\gamma=1$ ;  $\alpha=\gamma=1$  and  $\beta=2$ ;  $\alpha=\beta=1$  and  $\gamma=2$ ), which  
592 corresponds to the hypothesis of one dimension being more important than the others  
593 in the donor selection. There is very little effect on the number of target megafloods  
594 below the envelope (Extended Data Fig. 3). While a different set of parameters may  
595 modify some of the donor catchments, the resulting envelope curve changes very little.  
596 Finally we tested the effect of replacing the regional subdivision of Fig. 1 by an  
597 alternative subdivision<sup>17</sup>. The analysis shows that the alternative regions may modify  
598 the choice of individual donor catchments but, again, the overall conclusions do not  
599 change (Extended Data Fig. 4-7).

600

## 601 **Data availability**

602 The flood discharge data from the data holders/sources listed in Extended Data  
603 Table 1 that were used in this paper are available at  
604 <https://github.com/tuwhydro/megafloods>.

605

## 606 **Code availability**

607 The data analysis was performed in R using the supporting packages circular,  
608 lubridate, plotrix, quantreg, raster, RColorBrewer, rgdal, rworldmap and scales. The  
609 code used can be downloaded from <https://github.com/tuwhydro/megafloods>.

610

## 611 **Methods-only references**

612 32. Hall, J. et al. A European Flood Database: facilitating comprehensive flood research beyond  
613 administrative boundaries. Proc. Int. Assoc. Hydrol. Sci. 370, 89–95 (2015)

- 614 33. Roekaerts, M.: The biogeographical regions map of Europe, in: Basic principles of its creation  
615 and overview of its development, European Environment Agency, Copenhagen, available at:  
616 [https://www.eea.europa.eu/data-and-maps/ data/biogeographical-regions-europe-3](https://www.eea.europa.eu/data-and-maps/data/biogeographical-regions-europe-3) (2002).
- 617 34. Koenker, R. W. Quantile Regression, Cambridge U. Press (2005).
- 618 35. Amponsah, W., Marra, F., Marchi, L., Roux, H., Braud, I., Borga, M. Objective Analysis of  
619 Envelope Curves for Peak Floods of European and Mediterranean Flash Floods. In: Leal  
620 Filho, W., Nagy, G., Borga, M., Chávez Muñoz, P., Magnuszewski, A. (eds) Climate Change,  
621 Hazards and Adaptation Options. Climate Change Management. Springer, Cham (2020).
- 622 36. Tukey JW. Exploratory Data Analysis. Reading (Addison-Wesley): MA, 1977.
- 623 37. Hubert, M., & Vandervieren, E. (2008). An adjusted boxplot for skewed  
624 distributions. Computational statistics & data analysis, 52(12), 5186-5201.
- 625 38. Brys G, Hubert M, Struyf A. A robust measure of skewness. J. Comput. Graph. Stat. 2004;  
626 13: 996–1017.